

The role of asperity heterogeneity on the evolution of permeability creation during fault zone stimulation

EGU live chat, 07.05.2020, 14:00 – 15:45

Villiger, Linus; Zbinden, Dominik; Rinaldi, Antonio Pio; Selvadurai, Paul, Antony; Krietsch, Hannes; Gischtig, Valentin; Doetsch, Joseph; Jalali, Mohammadreza; Amann, Florian; Wiemer, Stefan

Key points

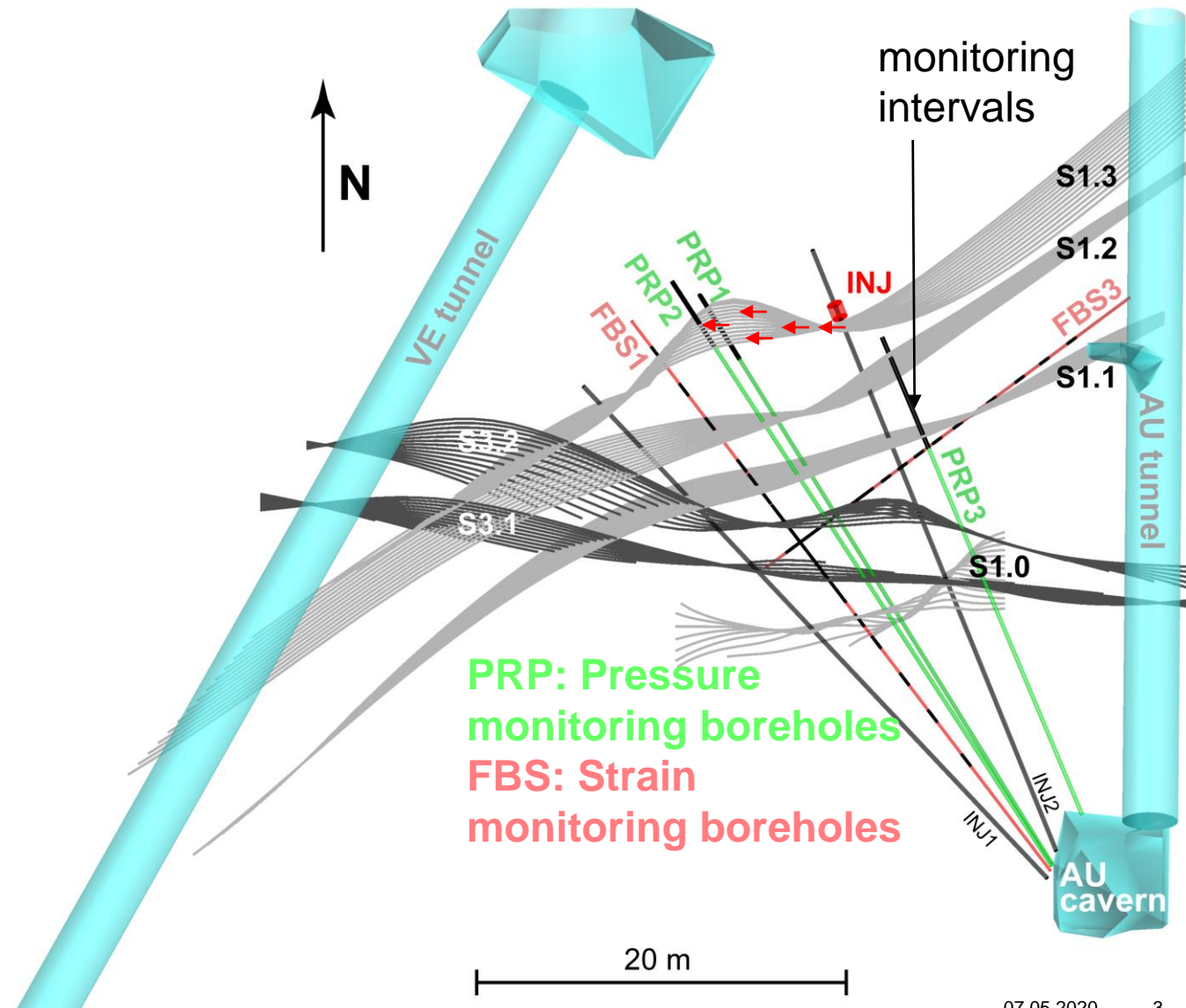
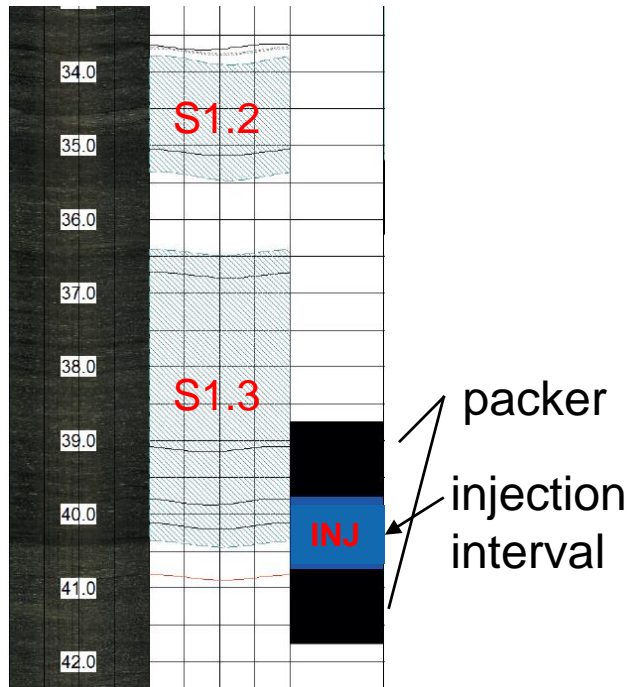
- We investigate observations from one high-pressure hydraulic stimulation experiment (denoted HS1)* performed on February 15th, 2017 using two-dimensional numerical modelling.
 - Target for high-pressure fluid injection was the originally ductile shear zone S1.3 at the Grimsel Test Site (GTS), Switzerland (slide 3).
 - Observed seismicity propagated in direction Up and West from the injection interval and was mostly confined to the target shear zone (slides 4, 5).
 - The highest spatial seismicity density was observed in Up and West direction corresponds to the most pronounced changes in seismic velocities and pressure signals suggested that permeability enhancement is highly localized and heterogeneous (slides 6, 7).
- We modelled the hydraulic behaviour using the TOUGH2-seed simulator, which couples the TOUGH2 fluid flow simulator with a stochastic seed model (Rinaldi and Nespoli, 2017). The model helps to explain the directionality of pressure fronts and induced seismicity observed during HS1 and other hydraulic stimulation experiments at the GTS (slides 8, 9).

* The experiment was part of the hydraulic stimulation experiments, jointly referred to as the In-situ Stimulation and Circulation (ISC) project executed at the Grimsel Test Site (GTS) in Switzerland (Amann et al., 2018; Doetsch et al., 2018).

Target S1.3 shear zone, strain and pressure monitoring

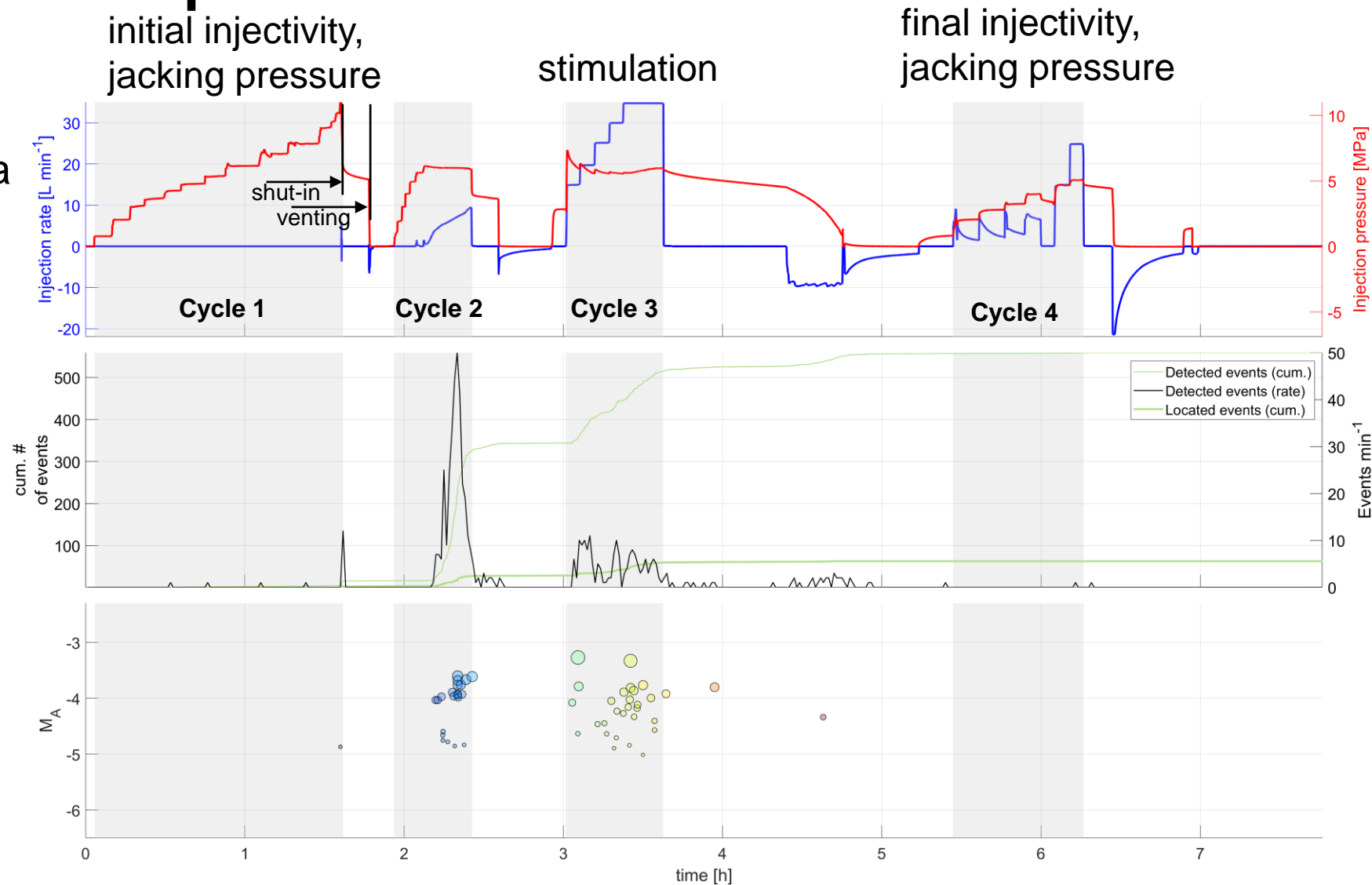
- The targeted, originally ductile S1.3 shear zone, striking NE-SW, contains a single fracture in the injection interval (**INJ**).

Borehole INJ2



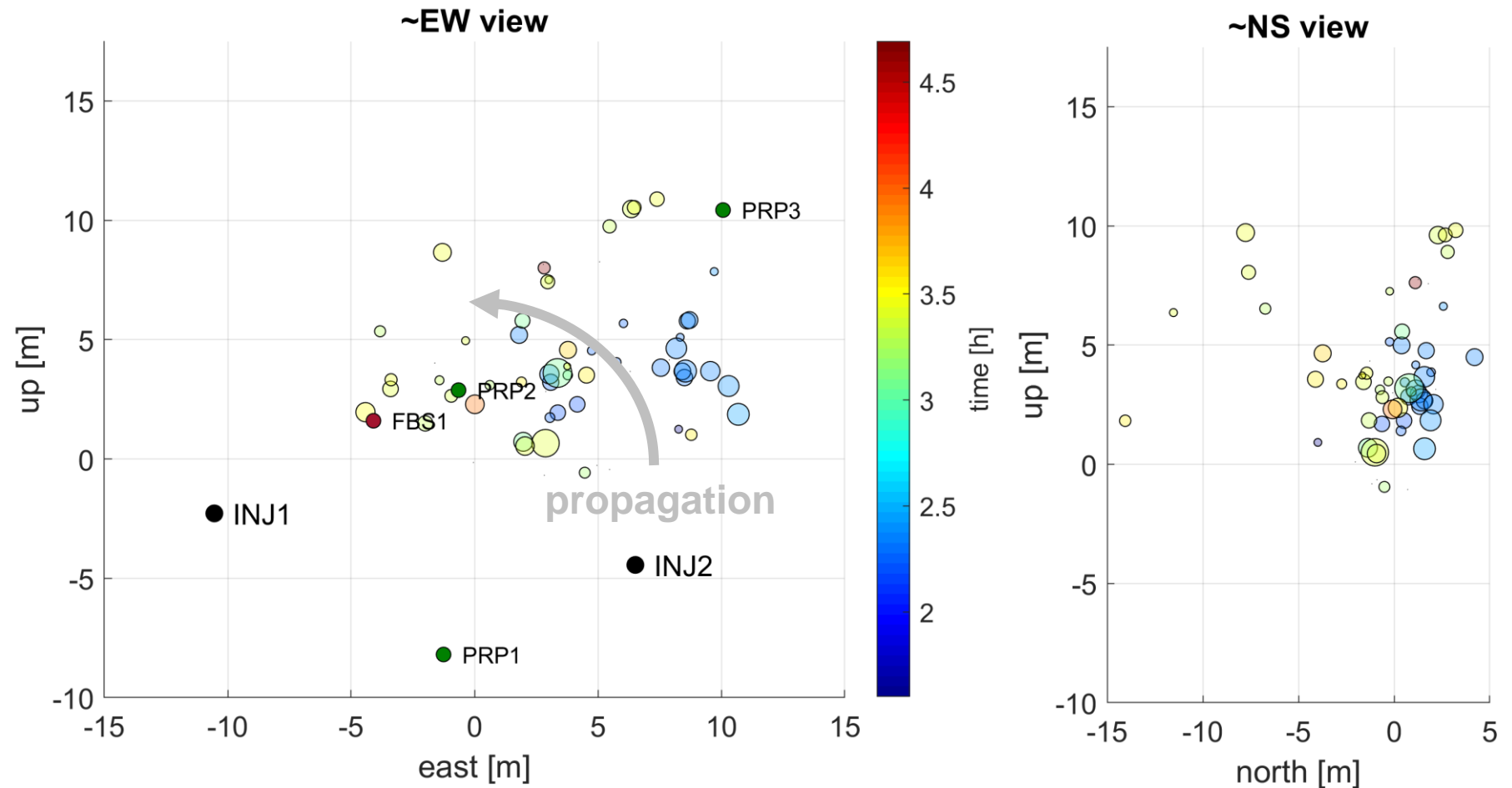
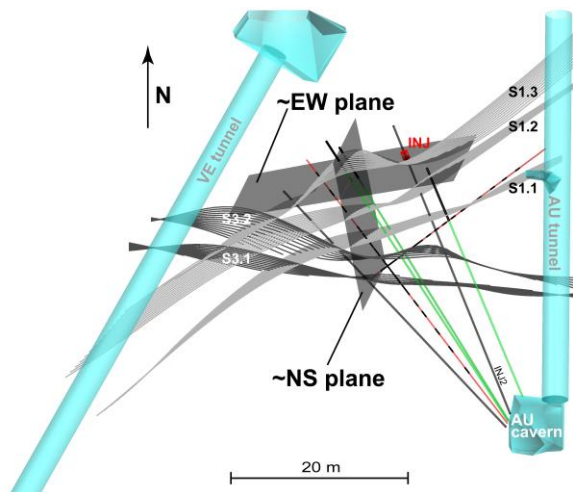
Seismicity evolution – temporal

- Injection protocol: 4 injection cycles flowed by a shut-in and venting phase
- Initially, we saw low connectivity between injection interval and present natural fracture network
- 559 seismic events were detected, 56 of the detections were successfully located



Seismicity collapsed to ~EW and ~NS planes

- Propagation of seismicity in direction Up and West, towards PRP2
- Some seismicity in adjacent shear zones S1.2, S1.1

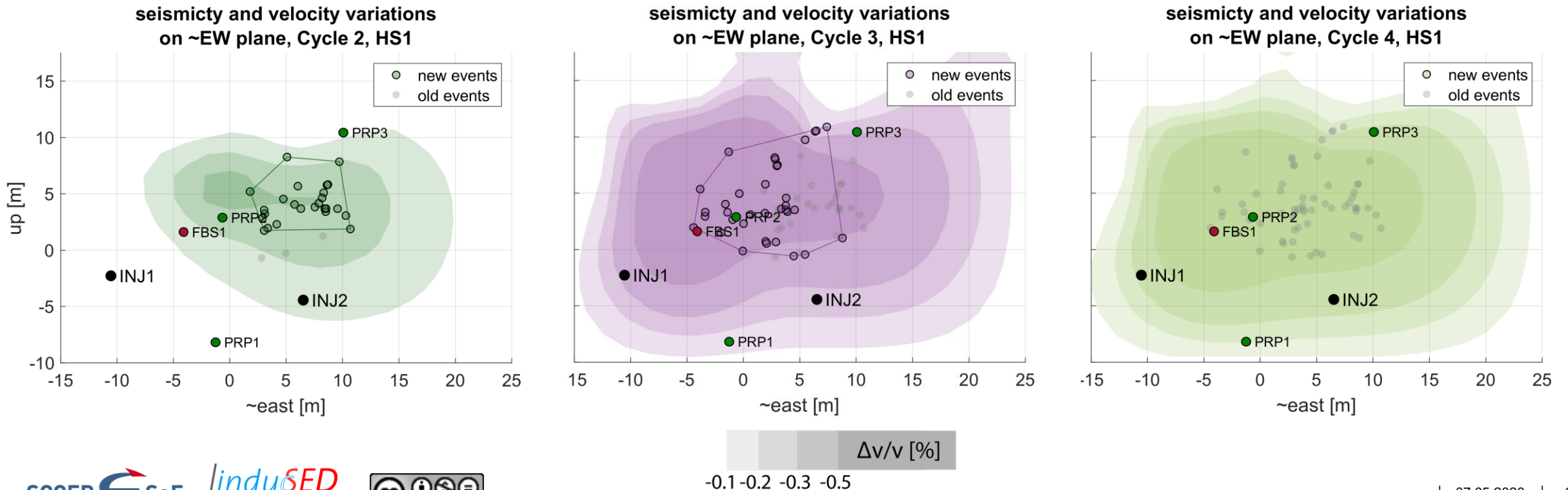


* ~EW plane is fitted through borehole observations of target shear zone S1.3. ~NS plane is perpendicular to ~EW plane

* Seismicity data is from Villiger et al., 2020

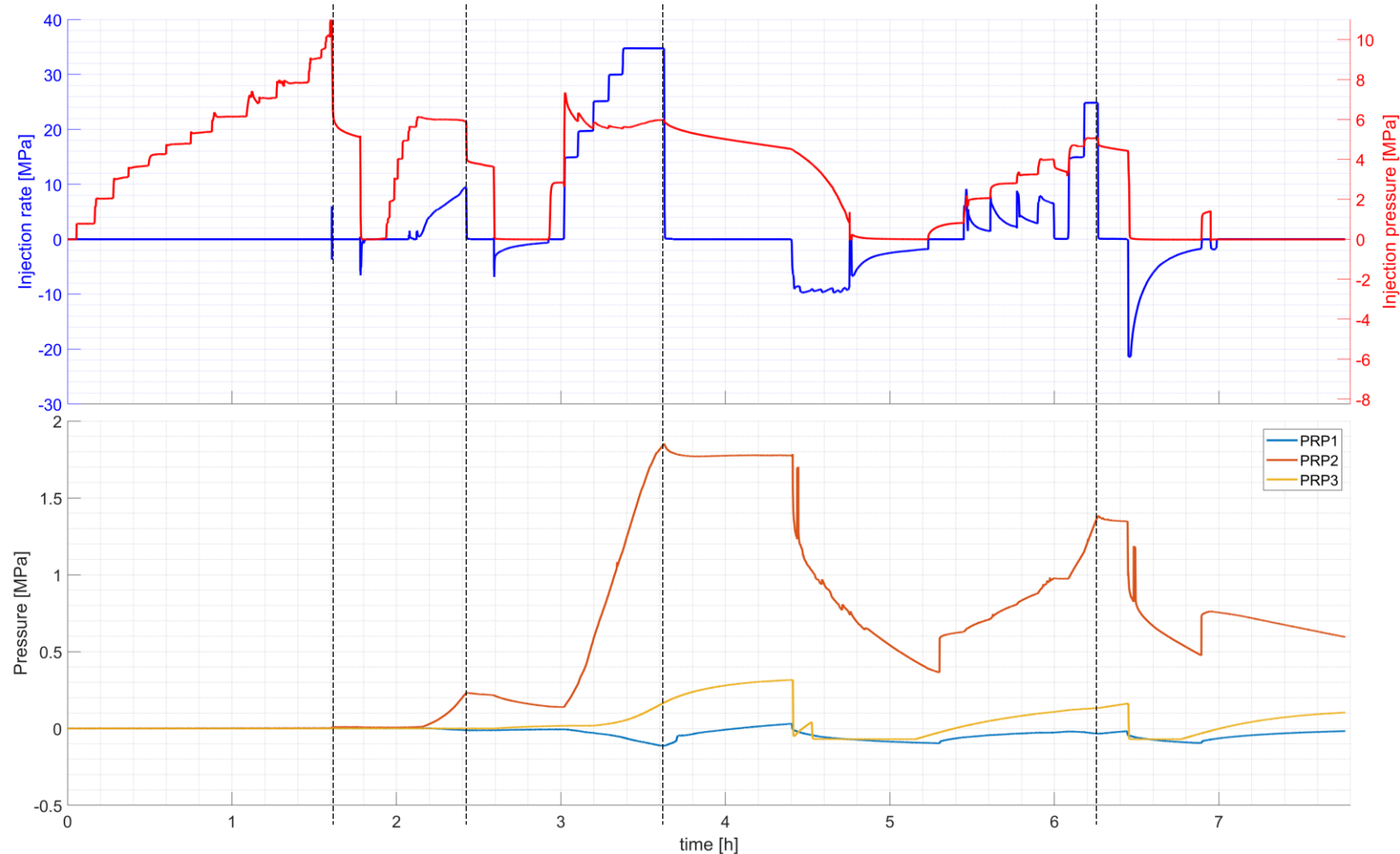
Seismicity and seismic velocity variations on ~EW plane

- Observed velocity variations (contour lines) at peak injection during cycle 2, 3, 4 and occurring located seismicity (seismic velocity variation data is taken from Schopper et al. (2020)).



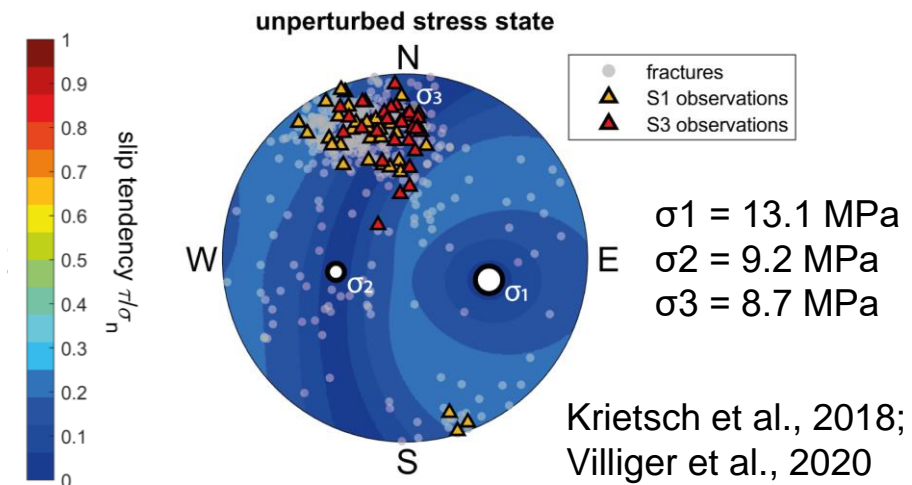
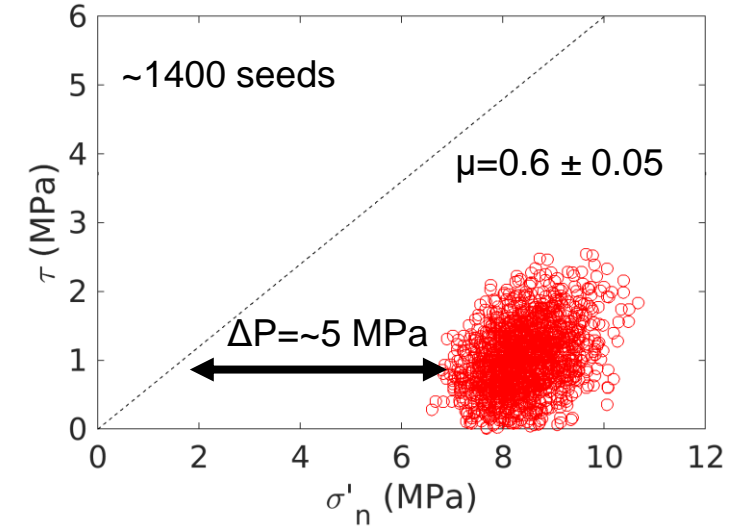
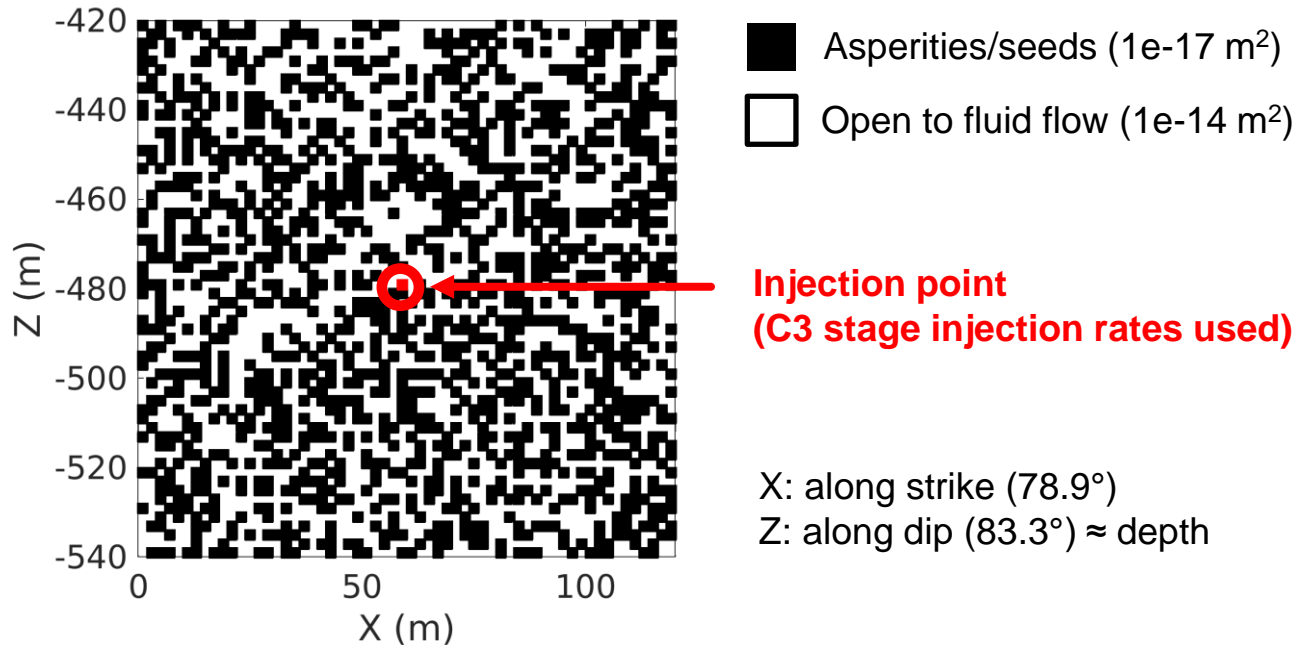
Pressure evolution in monitoring boreholes PRP1, 2, 3

- Strongest positive pressure signal measured in monitoring borehole PRP2 with correlating trend to injection parameters
- Monitored pressure in PRP2 remains at a high level also after shut-in suggesting closed, large pressurized volume



2D hydro-mechanical modeling with TOUGH2-seed

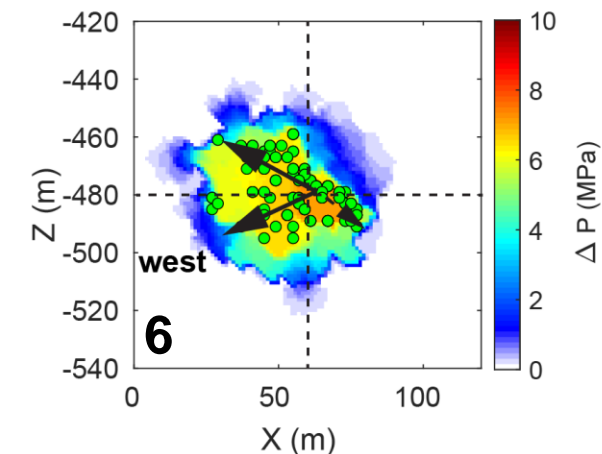
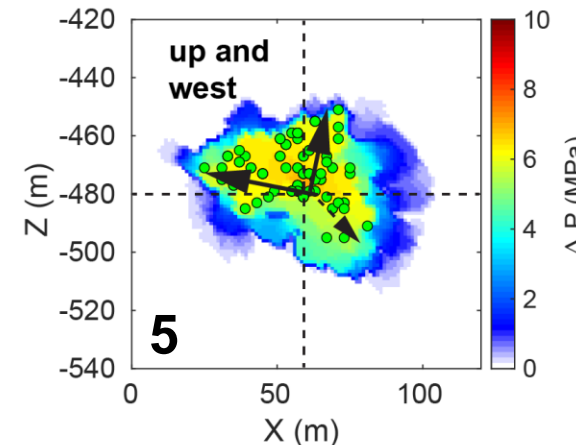
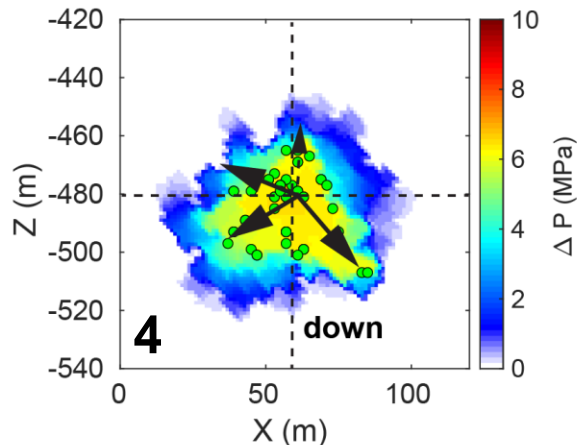
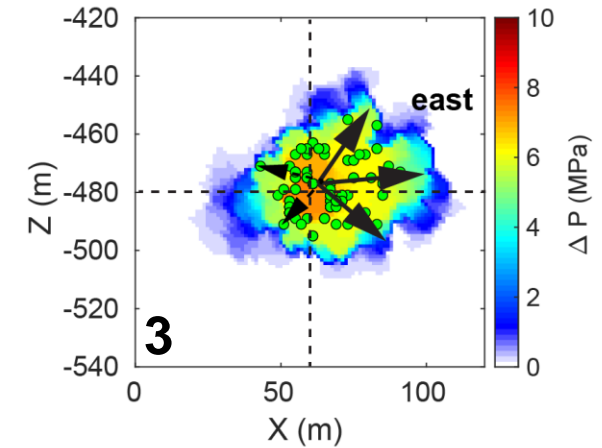
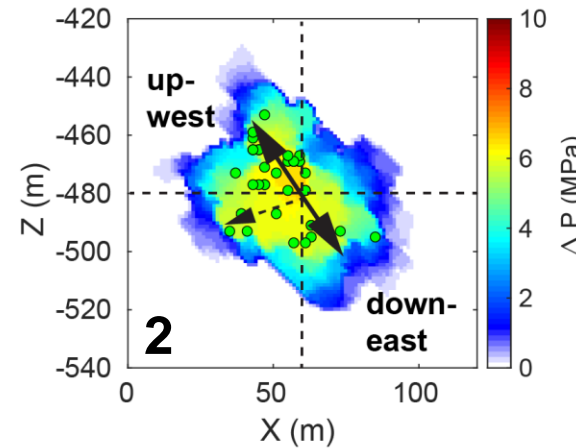
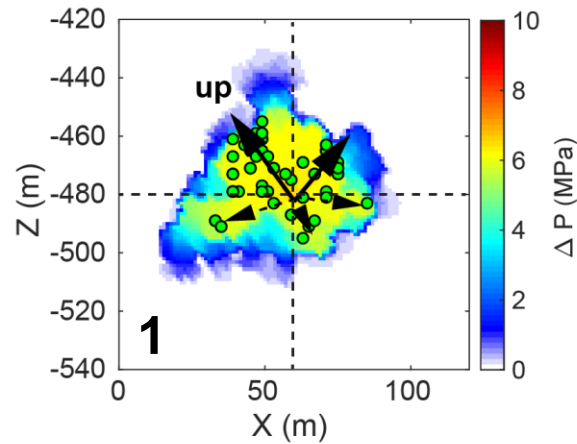
- Heterogeneous initial asperity (permeability) distribution (40% asperities)
- TOUGH2-seed (Rinaldi and Nespoli, 2017) allows to use a stochastic initial stress distribution
- Permeability change due to *elastic* normal deformation is simulated with the Barton-Bandis model (see appendix)



Krietsch et al., 2018;
Villiger et al., 2020

Main trends of pressure and seismicity for six random simulations

- Pressure and seismicity shown at shut-in time
- Each simulation shows different trends due to random initialization of permeability asperities
- Directionality of simulation #1 has some similarity to the HS1 experiment (migration trend, number of events, events after shut-in, see appendix for more details)



References

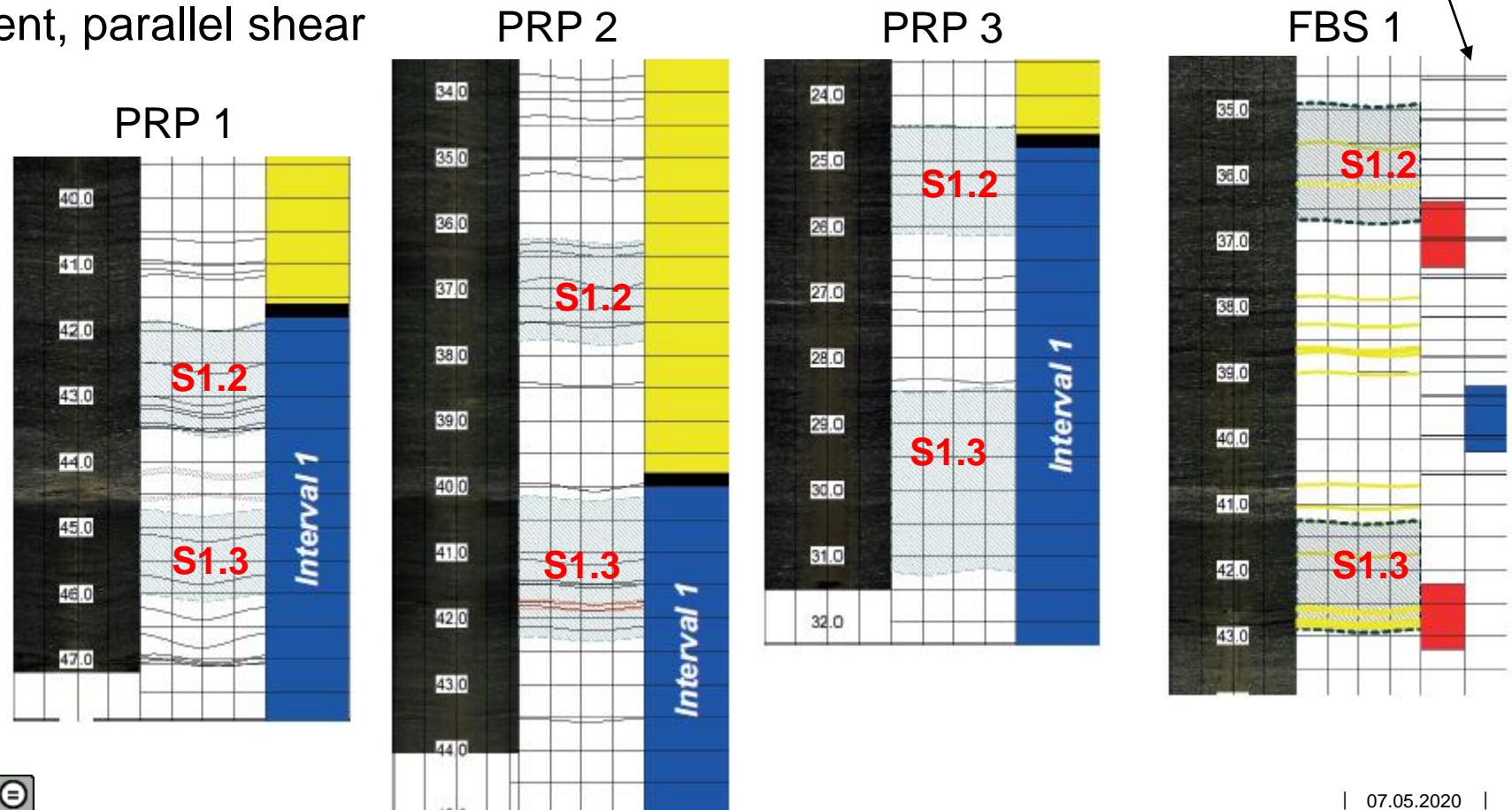
- Bandis, S., Lumsden, A., & Barton, N. (1983). Fundamentals of rock joint deformation. *International Journal of Rock Mechanics and Mining Science and Geomechanics Abstracts*, 20(6), 249–268. [https://doi.org/10.1016/0148-9062\(83\)90595-8](https://doi.org/10.1016/0148-9062(83)90595-8)
- Barton, N., Bandis, S., & Bakhtar, K. (1985). Strength, deformation and conductivity coupling of rock joints. *International Journal of Rock Mechanics and Mining Science and Geomechanics Abstracts*, 22(3), 121–140. [https://doi.org/10.1016/0148-9062\(85\)93227-9](https://doi.org/10.1016/0148-9062(85)93227-9)
- Doetsch, J., Gischig, V., Krietsch, H., Villiger, L., Amann, F., Dutler, N., . . . Hochreutener, R. (2018). Grimsel ISC Experimental Description. doi:<https://doi.org/10.3929/ethz-b-000310581>
- Krietsch, H., Gischig, V., Evans, K., Doetsch, J., Dutler, N. O., Valley, B., & Amann, F. (2018). Stress Measurements for an In Situ Stimulation Experiment in Crystalline Rock: Integration of Induced Seismicity, Stress Relief and Hydraulic Methods. *Rock Mechanics and Rock Engineering*, 1-26.
- Krietsch, H., Gischig, V., Doetsch, J., Evans, K. F., Villiger, L., Jalali, M. R., . . . Amann, F. (in review, 2019). Hydro-mechanical processes and their influence on the stimulated volume: Observations from a decameter-scale hydraulic stimulation experiment. *Solid Earth Discuss.* doi:<https://doi.org/10.5194/se-2019-204>
- Krietsch, H., Villiger, L., Doetsch, J., Gischig, V., Evans, K. F., Brixel, B., . . . Amann, F. (2020). Changing flow paths caused by simultaneous shearing and fracturing observed during hydraulic stimulation. *Geophysical Research Letters*, 47(3), e2019GL086135.
- Rinaldi, A. P., & Nespoli, M. (2017). TOUGH2-seed: A coupled fluid flow and mechanical-stochastic approach to model injection-induced seismicity, *Computers and Geosciences*, 108, 86–97, <https://doi.org/10.1016/j.cageo.2016.12.003>
- Schopper, F., Doetsch, J., Villiger, L., Krietsch, H., Gischig, V. S., Jalali, M., . . . Maurer, H. (2020). On the Variability of Pressure Propagation during Hydraulic Stimulation based on Seismic Velocity Observations. *Journal of Geophysical Research: Solid Earth*. doi:<https://doi.org/10.1029/2019JB018801>
- Ucar, E., Berre, I., & Keilegavlen, E. (2018). Three-dimensional numerical modeling of shear stimulation of fractured reservoirs. *Journal of Geophysical Research: Solid Earth*, 123. <https://doi.org/10.1029/2017JB015241>
- Villiger, L., Gischig, V., Doetsch, J., Krietsch, H., Dutler, N., Jalali, M. R., . . . Wiemer, S. (2020). Influence of reservoir geology on seismic response during decameter scale hydraulic stimulations in crystalline rock. *Solid Earth*, 11(2), 627-655. doi:<https://doi.org/10.5194/se-11-627-2020>

Appendix

Monitoring intervals – strain, pressure

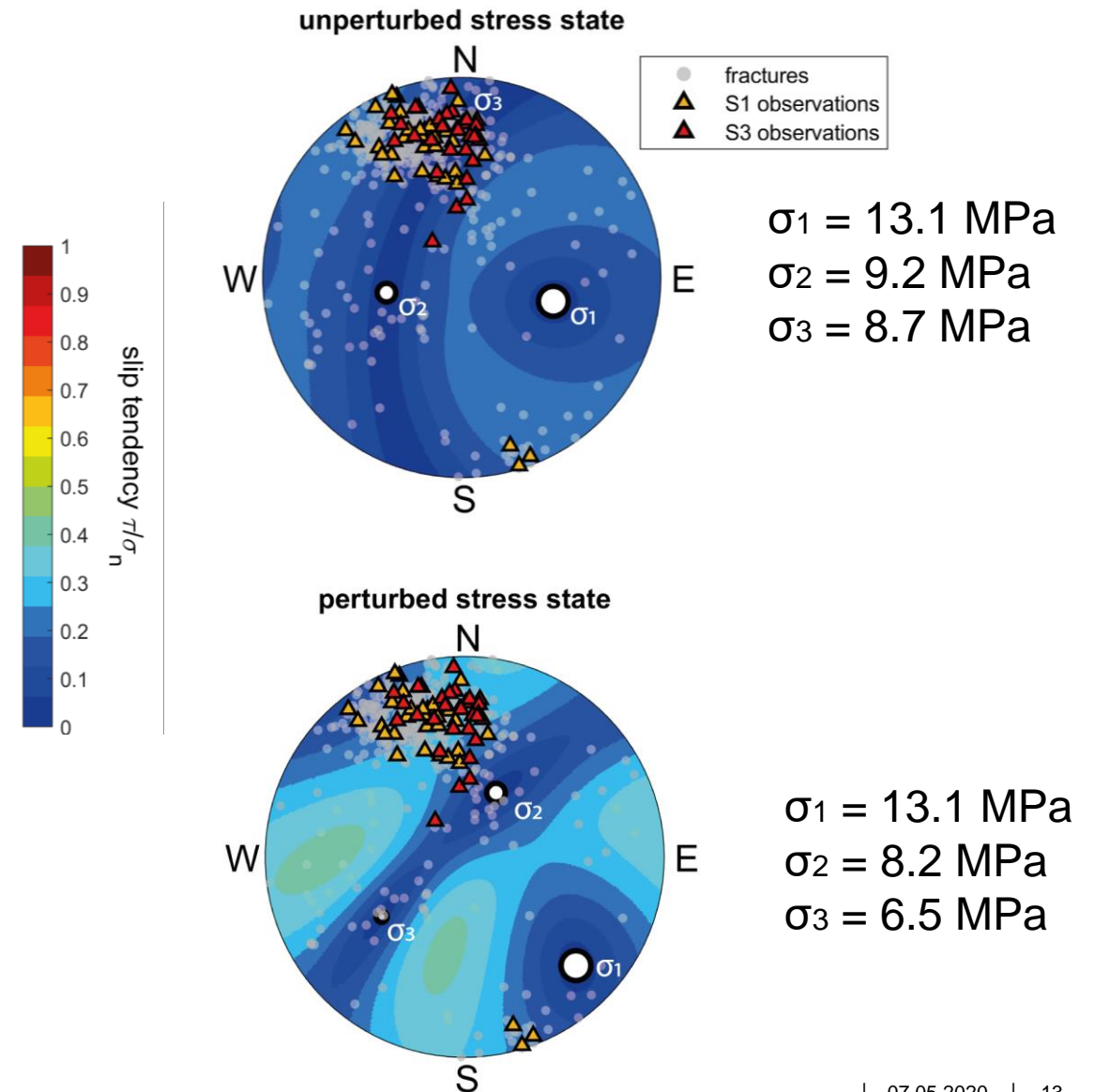
- The monitoring intervals in the respective monitoring boreholes can span over shear zone S1.3 and the adjacent, parallel shear zone S1.2.

Grouted longitudinal strain sensors of 1 m length



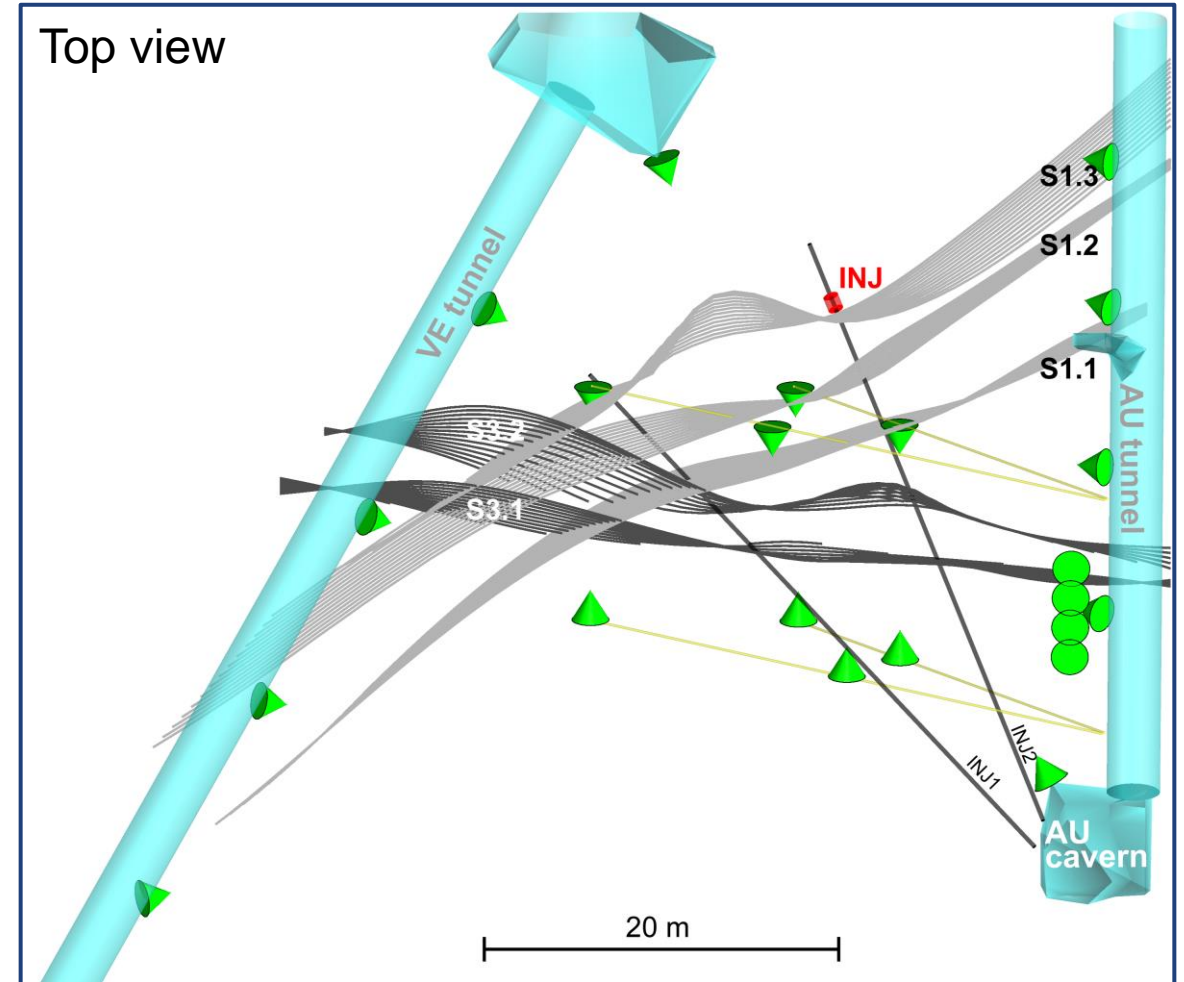
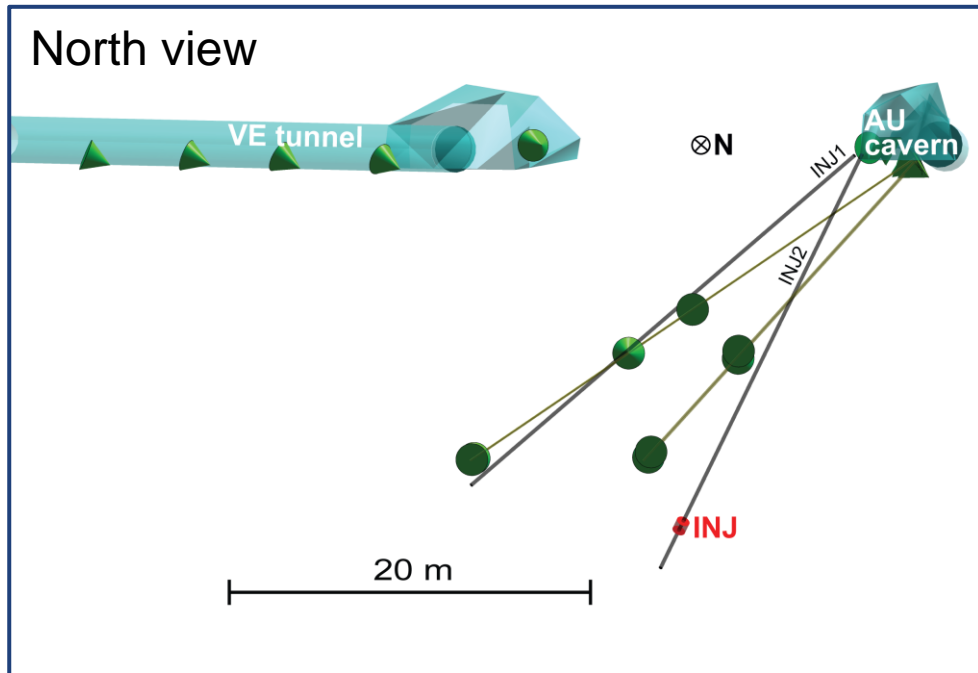
Stress state, slip tendencies

- Stress measurements at two locations in the experimental volume (Krietsch et al., 2018).
 - The **unperturbed stress state** was measured 30 m south of the S3 shear zones, unaffected by the shear zones.
 - The **perturbed stress state** was measured at the S3.1 shear zone in the south of the experimental volume
 - The stress state directly at the target shear zone S1.3 is not known.



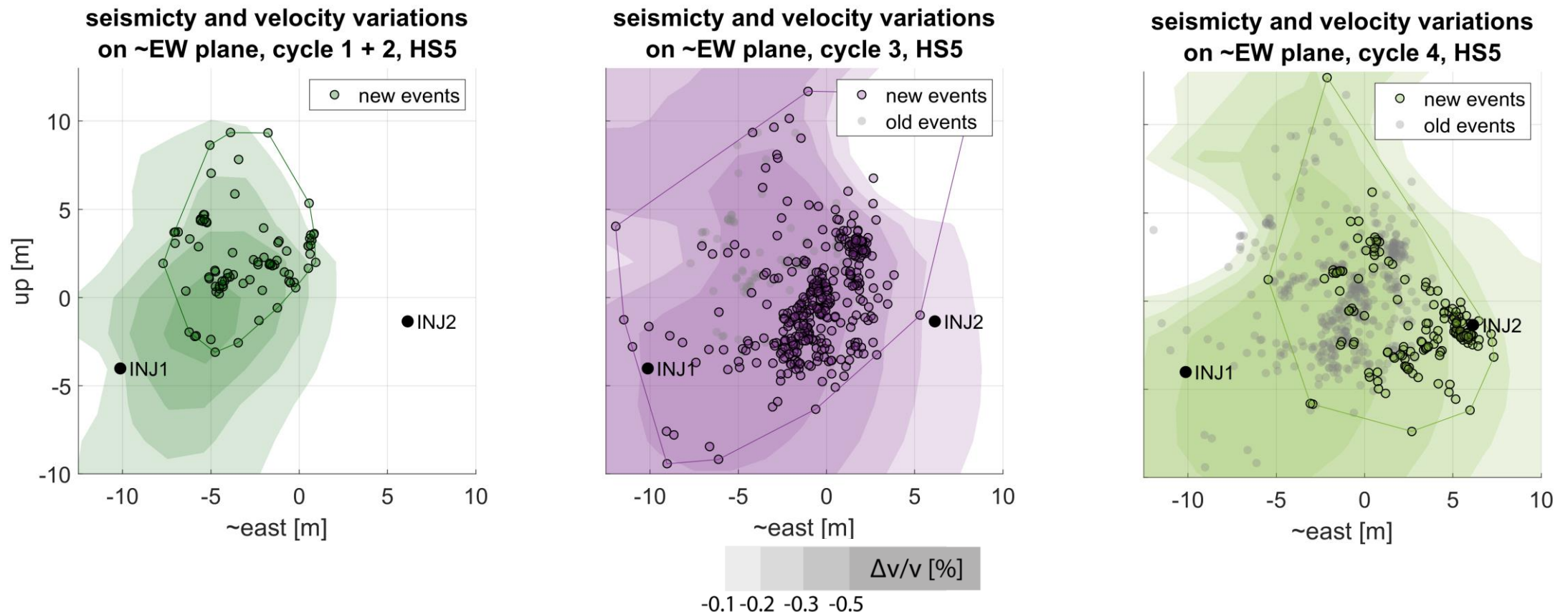
Seismic monitoring network

- 26 uncalibrated acoustic emission sensor (AE, green cones)
- Core network: 8 AE's installed in boreholes in close vicinity to injection (**injection outside core network**)



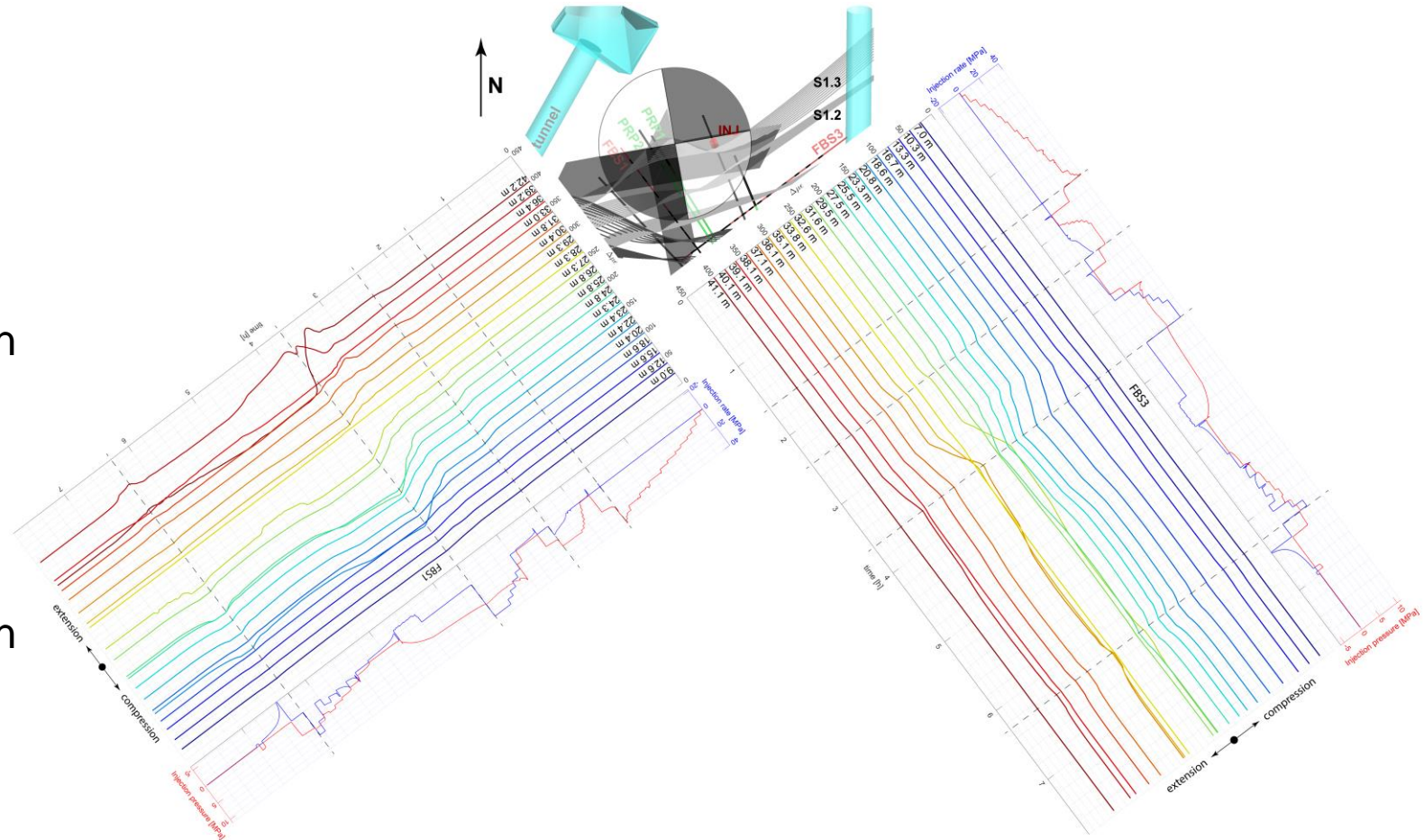
Additional experiment (HS5*) showing seismicity evolution and velocity variations in different direction compared to HS1

- During experiment HS5 injection borehole INJ1 is hydraulically connected to borehole INJ2



Strain evolution in borehole FBS1 and FBS3

- FBS1 (perpendicular to target shear zone S1.3):
 - mostly compressional signals observed
 - at the level of S1.3 complex varying signals from compression to extension
- FBS3 (parallel to target shear zone S1.3):
 - extensional signals in the upper part and compressional signals in the lower part of the borehole suggests tensional and compressional lobe of strike-slip movement at the target shear zone.

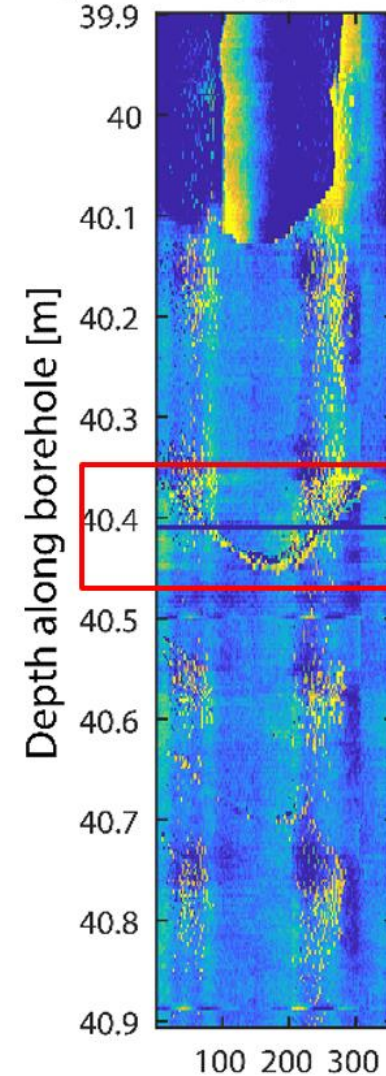


Injection interval properties

- Injectivity change
 - Injectivity (cycle 2): 0.0006 l/min/MPa
 - Injectivity (cycle 4): 1.11 l/min/MPa
- Interval transmissivity change (pulse tests)
 - Pre stimulation: $8.3e-11$ m²/s
 - Post stimulation: $1.5e-7$ m²/s
- Slip displacement measured through difference image of acoustic televiewer (ATV) logs recorded pre and post stimulation: 0.75 mm

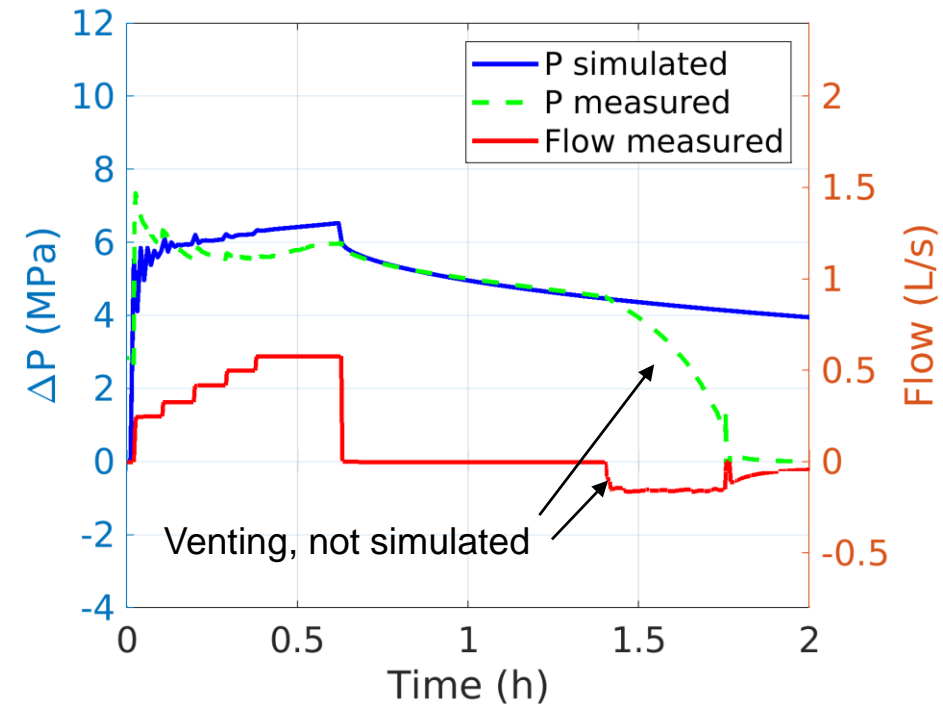
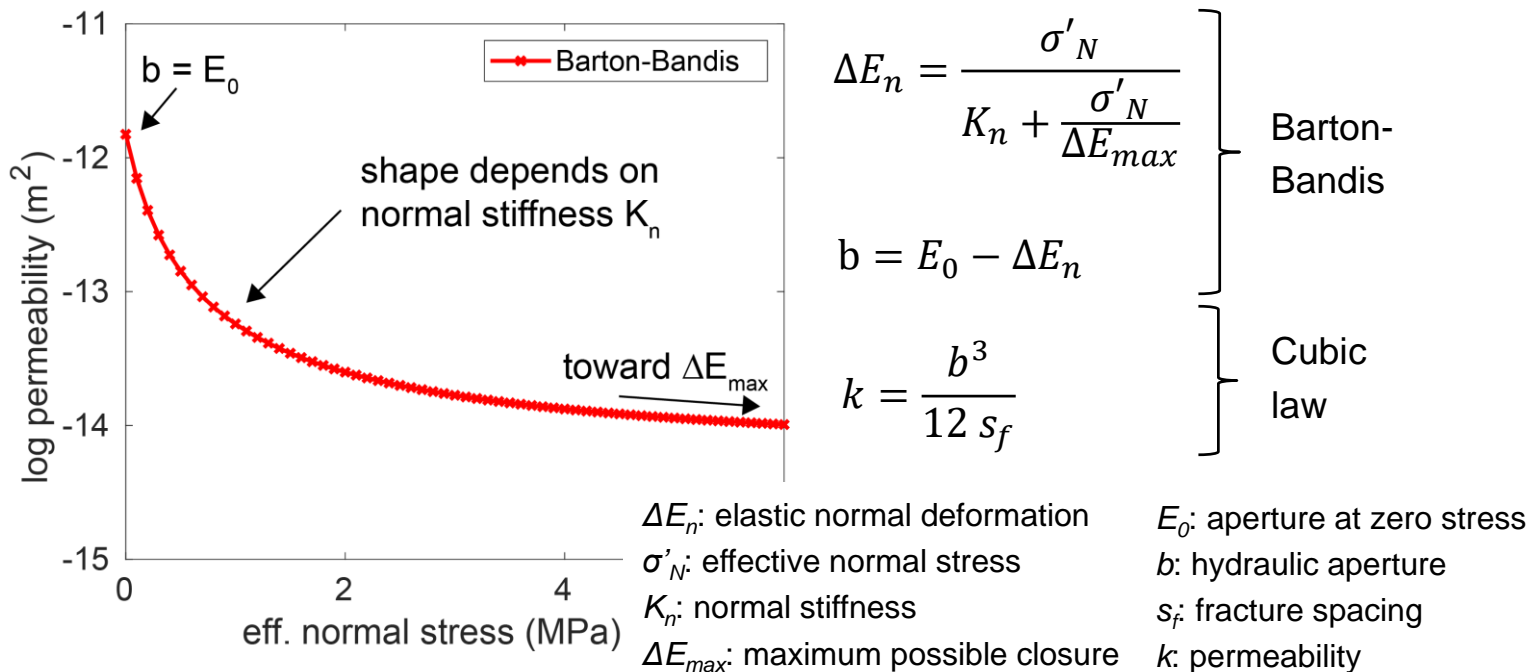
(these data is beeing publisched in Krietsch et al., in review, 2019)

Differences in ATV logs



Modeling: Elastic fracture opening

- Permeability change due to *elastic* normal deformation is simulated with the Barton-Bandis model (Bandis et al., 1983; Barton et al., 1985; see also Ucar et al., 2018)
- Here, the aim is not to achieve a perfect match between the measured and simulated pressure, but rather to obtain approx. the maximum pressure change and a good fit of the shut-in behavior.



Directed propagation of pressure and seismicity due to asperities: Simulation #1

Some observations similar to HS1:

- Most pressure change and seismicity occurs above injection point
- Little seismicity simulated after shut-in ($t > 0.62$ hours) – only very few events in HS1 after shut-in
- 68 simulated events (56 located events in HS1 – Villiger et al., 2020)

